

Characterizing N -dimensional anisotropic Brownian motion by the distribution of diffusivities

Mario Heidernätsch, Michael Bauer, and Günter Radons*

Chemnitz University of Technology, Faculty of Natural Sciences, Institute of Physics, Complex Systems and Nonlinear Dynamics, D-09107 Chemnitz, Germany

(Dated: July 1, 2022)

Anisotropic diffusion processes emerge in various fields such as transport in biological tissue and diffusion in liquid crystals. In such systems, the motion is described by a diffusion tensor. For a proper characterization of processes with more than one diffusion coefficient an average description by the mean squared displacement is often not sufficient. Hence, in this paper, we use the distribution of diffusivities to study diffusion in a homogeneous anisotropic environment. We derive analytical expressions of the distribution and relate its properties to an anisotropy measure in order to distinguish between isotropic and anisotropic processes. We further discuss the influence on the analysis of projected trajectories, which are typically accessible in experiments. For the experimentally relevant cases of two- and three-dimensional anisotropic diffusion we derive the specific expressions, determine the diffusion tensor, characterize the anisotropy, and demonstrate the applicability for simulated trajectories.

PACS numbers: 05.40.-a, 02.50.-r, 87.80.Nj

Keywords: anisotropic systems, diffusion, distribution of diffusivities

I. INTRODUCTION

The random motion of suspended particles in a fluid, which is usually referred to as Brownian motion, is an old but still fascinating phenomenon. Especially, when inhomogeneous [1–3] or anisotropic media [4–6] are involved, a lot of questions are still open. From the theoretical point of view, a lot of work has been done [7] to predict the statistical properties of the trajectories of such particles using stochastic methods. On the contrary, the development of experiments only recently allows obtaining the paths of individual molecules and particles. Especially the observation of two-dimensional trajectories using video-microscopic methods, for instance single-particle tracking (SPT), is already successfully applied in biological systems [8, 9] or to understand the microrheological properties of complex liquids [10, 11]. But also the observation of three-dimensional paths becomes feasible [12–14]. The statistical analysis of these trajectories is usually accomplished by measuring the mean square displacement (msd) in order to get the diffusion coefficients for the matching theoretical description. However, in the anisotropic case the diffusive properties depend on the direction of motion and are described by a diffusion tensor. In such systems, the analysis of msds turned out to be not sufficient to determine the anisotropy and extract the values of the diffusion coefficients [15–17]. For similar reasons, we already introduced the distribution of single-particle diffusivities as an advanced method to analyze stochastic motion in heterogeneous systems [18] involving more than one diffusion coefficient.

In the current article, we show the applicability of the distribution of diffusivities to analyze trajectories of ho-

mogeneous anisotropic Brownian motion. We present the properties of the distribution as well as their relations to established quantities. In order to assess the parameters of the process, we calculate the characteristic function, cumulants and moments of the distribution. For the asymptotic decay of the distribution of diffusivities, we derive a general expression, which involves the largest diffusion coefficient of the system. In conjunction with the mean diffusion coefficient of the system, the asymptotic decay enables a distinction between isotropic and anisotropic processes. Based on these quantities, we provide a measure to characterize the anisotropy of the process from the analysis of SPT data. Since in experiments the reconstruction of the complete diffusion tensor is of great interest, we extend our concept to tensorial diffusivities, which offer a simple method to determine the entries of the tensor.

Due to restrictions in SPT experiments the complete trajectory is often not accessible [4, 19]. Hence, we investigate the influence on the distribution of diffusivities and the detection of the anisotropy if only projections of the actual trajectory are observed. Even in such cases it is possible to estimate bounds of the diffusion coefficients from the given projections of the diffusion tensor. Since especially two-dimensional and three-dimensional diffusion processes have a high relevance in experiments we apply our considerations to these systems. For homogeneous anisotropic diffusion in two dimensions an analytical expression of the distribution of diffusivities exists and its moments can be related to the diffusion coefficients, which enter the anisotropy measure. Moreover, we explain the details to reconstruct the diffusion tensor from the tensorial diffusivities as well as from projections of the trajectory. Three-dimensional processes are investigated analogously although a closed-form expression of the distribution of diffusivities does not exist. Addition-

* radons@physik.tu-chemnitz.de

ally, we deal with anisotropic processes where one diffusion coefficient is degenerated corresponding to diffusion of uniaxial molecules typical for liquid crystalline systems [20].

The paper is organized as follows. In Sec. II, we briefly recall the theoretical principles of anisotropic Brownian motion based on the diffusion tensor and introduce the distribution of single-particle diffusivities, its properties and relations to established quantities. To apply our new concepts to N -dimensional homogeneous anisotropic diffusion processes, we provide in Sec. III a general expression for the distribution of diffusivities. We demonstrate how to distinguish between isotropic and anisotropic processes and explain the reconstruction of the diffusion tensor. Since in experiments the complete trajectory is often not accessible, we investigate in Sec. IV how projections of the trajectory influence the distribution of diffusivities. Finally, in Sec. V, we apply our results to specific systems of anisotropic diffusion which are typical for experimental setups. We substantiate the applicability of our findings by analyzing data from simulated anisotropic diffusion processes.

II. DEFINITIONS

A. Anisotropic diffusion

An N -dimensional anisotropic Brownian motion is completely defined by its propagator [21]

$$p(\mathbf{x}, t | \mathbf{x}', t') = \frac{(2\pi)^{-\frac{N}{2}}}{\sqrt{[2(t-t')]^N \det \mathbf{D}}} \times \exp \left[-\frac{1}{2} \frac{1}{2(t-t')} (\mathbf{x} - \mathbf{x}')^\top \mathbf{D}^{-1} (\mathbf{x} - \mathbf{x}') \right] \quad (1)$$

where $\mathbf{D} = \mathbf{O}^\top \hat{\mathbf{D}} \mathbf{O}$ is the positive definite and symmetric diffusion tensor, $\hat{\mathbf{D}} = \text{diag}(D_1, D_2, \dots, D_N)$ denotes its diagonalized form with the diffusion coefficients D_i belonging to the principal axes, and \mathbf{O} is an orthogonal tensor which describes the orientation of the principal axes relative to the frame of reference.

For the simulation of such processes an alternative description exists, where the propagator corresponds to the Langevin equation

$$\frac{d\mathbf{x}}{dt} = \sqrt{2\mathbf{D}} \boldsymbol{\xi}(t) \quad (2)$$

with $\sqrt{\mathbf{D}} = \mathbf{O}^\top \sqrt{\hat{\mathbf{D}}} \mathbf{O}$ and $\sqrt{\hat{\mathbf{D}}} = \text{diag}(\sqrt{D_1}, \sqrt{D_2}, \dots, \sqrt{D_N})$. The vector $\boldsymbol{\xi}(t) = [\xi_1(t), \dots, \xi_N(t)]^\top$ denotes Gaussian white noise in N dimensions with $\langle \boldsymbol{\xi}(t) \rangle = \mathbf{0}$ and $\langle \xi_i(t) \xi_j(t') \rangle = \delta_{ij} \delta(t-t') \forall i, j \in \{1, 2, \dots, N\}$.

Assuming time-translation invariance and considering displacements Eq. (1) is simplified to $p(\mathbf{x}' + \mathbf{r}, \tau | \mathbf{x}')$ by

substituting $\tau = t - t'$ and $\mathbf{r} = \mathbf{x} - \mathbf{x}'$. This conditional probability density is averaged by the equilibrium distribution $p_0(\mathbf{x}')$ given by the Boltzmann distribution to obtain the ensemble-averaged stationary probability density

$$p(\mathbf{r}, \tau) = \int d^N \mathbf{x}' p(\mathbf{x}' + \mathbf{r}, \tau | \mathbf{x}') p_0(\mathbf{x}') = \frac{(2\pi)^{-\frac{N}{2}}}{\sqrt{\det \Sigma}} \exp \left(-\frac{1}{2} \mathbf{r}^\top \Sigma^{-1} \mathbf{r} \right) \quad (3)$$

of a displacement $\mathbf{r} = (r_1, \dots, r_N)^\top$ in the time interval τ . Thus, $p(\mathbf{r}, \tau)$ is an N -dimensional Gaussian distribution with zero mean and covariance tensor $\Sigma = 2\tau\mathbf{D}$.

B. Distribution of diffusivities

By observing a trajectory $\mathbf{x}(t)$ of an arbitrary stochastic process in N dimensions individual displacements during a given time lag τ can simply be measured for a certain particle. Moreover, it is natural to relate each displacement to a single-particle diffusivity

$$D_t(\tau) = \frac{[\mathbf{x}(t + \tau) - \mathbf{x}(t)]^2}{2N\tau}. \quad (4)$$

This simple transformation of displacements to diffusivities offers the advantage to compare these quantities for different experimental setups and different τ . Since for a fixed time lag τ the single-particle diffusivity is fluctuating along a trajectory an important quantity is given by the probability density $p(D)$. Therefore, the distribution of single-particle diffusivities [18] is defined as

$$p(D, \tau) = \langle \delta [D - D_t(\tau)] \rangle, \quad (5)$$

where $\langle \dots \rangle$ either denotes a time average $\langle \dots \rangle = \lim_{T \rightarrow \infty} 1/T \int_0^T \dots dt$, which is typically accessible by SPT, or an ensemble average from different experimental methods, such as nuclear magnetic resonance [22]. For ergodic systems, as considered here, time average and ensemble average coincide. It should be noted that other definitions of diffusivity distributions exist in the literature [23].

For homogeneous systems, i.e., the distribution of displacements $p(\mathbf{r}, \tau)$ is independent of t , Eq. (5) is rewritten as

$$p(D, \tau) = \int d^N \mathbf{r} \delta \left(D - \frac{\mathbf{r}^2}{2N\tau} \right) p(\mathbf{r}, \tau) \quad (6)$$

transforming $p(\mathbf{r}, \tau)$ into the distribution of diffusivities.

For data from SPT experiments, $p(\mathbf{r}, \tau) = \langle \delta[\mathbf{r} - \mathbf{r}(\tau)] \rangle$ and the distribution of diffusivities is obtained by binning diffusivities into a normalized histogram according to Eq. (5). The normalization ensures that the histogram becomes an estimate of the probability density function.

For homogeneous isotropic processes in N dimensions the msd grows linearly with τ , since it obeys the well-known Einstein relation $\langle r^2(\tau) \rangle = 2ND_c\tau$, where D_c is the diffusion coefficient of the process. Due to the transformation of displacements to diffusivities by Eq. (4) the linear dependence on τ is removed. Hence, the corresponding distribution of diffusivities becomes stationary and comprises single-particle diffusivities fluctuating around D_c . For N -dimensional homogeneous isotropic processes the distribution of diffusivities

$$p_{D_c}^{Nd}(D) = \left(\frac{N}{2D_c} \right)^{\frac{N}{2}} \frac{D^{\frac{N}{2}-1}}{\Gamma(\frac{N}{2})} \exp\left(-\frac{N}{2D_c}D\right) \quad (7)$$

is obtained, where $\Gamma(x)$ denotes the gamma function. More generally, for normal diffusion in N dimensions the Einstein relation holds for large τ . In this case, D_c is the mean diffusion coefficient of the process. Hence, the distribution of diffusivities also converges to the stationary distribution given by Eq. (7) for homogeneous processes, which offers a further advantage of this distribution.

C. Moments

The distribution of diffusivities is fully characterized by its corresponding moments

$$M_m = \langle D(\tau)^m \rangle = \int_0^\infty dD D^m p(D, \tau). \quad (8)$$

It should be noted that the first moment is known as the mean diffusion coefficient, which is obtained by a well-defined integration. This is in contrast to msd measurements, where the mean diffusion coefficient is determined by a numerical fit to the slope of the msd. By inserting Eq. (6) into Eq. (8) the integration of D is accomplished. As a result the moments

$$\begin{aligned} M_m &= \frac{1}{(2N\tau)^m} \int d^N \mathbf{r} \mathbf{r}^{2m} p(\mathbf{r}, \tau) \\ &= (2N\tau)^{-m} \langle \mathbf{r}^{2m} \rangle \end{aligned} \quad (9)$$

are directly related to the moments of the distribution of displacements and, thus, to the moments of the propagator $p(\mathbf{x}, t | \mathbf{x}', t')$.

III. PROPERTIES OF THE DISTRIBUTION OF DIFFUSIVITIES FOR HOMOGENEOUS ANISOTROPIC BROWNIAN MOTION

A. Distribution of diffusivities

For homogeneous anisotropic diffusion in N dimensions, where $p(\mathbf{r}, \tau)$ is a Gaussian distribution with zero mean given by Eq. (3), the computation of the distribution of diffusivities, its moments, or its characteristic function is simplified by reformulating the integral of

Eq. (6). Applying the coordinate transform of $\mathbf{r} = \mathbf{Q}\mathbf{q}$ with $\mathbf{Q} = \sqrt{2\tau} \mathbf{O}^\top \sqrt{\mathbf{D}}$ results in the distribution of diffusivities

$$\begin{aligned} p_{\mathbf{D}}^{Nd}(D) &= \int dq_1 \cdots \int dq_N \\ &\times \delta \left(D - \frac{1}{N} \sum_{i=1}^N D_i q_i^2 \right) \prod_{j=1}^N p_{(0,1)}(q_j), \end{aligned} \quad (10)$$

where $p_{(0,1)}(q_j) = \frac{1}{\sqrt{2\pi}} \exp(-\frac{1}{2}q_j^2)$. Thus, the distribution of diffusivities is calculated by integration over independent standard normally distributed variables with zero mean and unit variance. Since the msd for homogeneous anisotropic diffusion again grows linearly as in the homogeneous isotropic case, the τ dependency in the distribution of diffusivities vanishes.

By obtaining the distribution of diffusivities, for instance, from displacements along a single trajectory, information about the orientation of the diffusion tensor is lost. However, all directions contribute to the distribution and, thus, it still contains information about the diffusion coefficients corresponding to the principal axes, i.e., the eigenvalues of \mathbf{D} .

B. Characteristic function, cumulants and moments

With the transformation Eq. (10), the moments and the characteristic function of the distribution of diffusivities of anisotropic Brownian motion are calculated. For the moments, given by Eq. (8), this yields

$$M_m^{Nd} = \frac{1}{N^m} \int dq_1 \cdots \int dq_N \left(\sum_{i=1}^N D_i q_i^2 \right)^m \prod_{j=1}^N p_{(0,1)}(q_j). \quad (11)$$

So, for instance, the first moment of the distribution of diffusivities is given by

$$M_1^{Nd} = \frac{1}{N} \sum_{i=1}^N D_i = \langle D(\tau) \rangle, \quad (12)$$

which is simply the arithmetic mean of all the diffusion coefficients D_i and coincides with the slope of the msd. For higher moments of the distribution of diffusivities, it is easier to calculate its characteristic function $G_{\mathbf{D}}^{Nd}(k) = \langle \exp(ikD) \rangle = \int_0^\infty dD \exp(ikD) p_{\mathbf{D}}^{Nd}(D)$ by substituting $p_{\mathbf{D}}^{Nd}(D)$ with Eq. (10) and performing the Fourier transform to obtain

$$\begin{aligned} G_{\mathbf{D}}^{Nd}(k) &= \prod_{j=1}^N \int dq_j \exp\left(ik \frac{D_j q_j^2}{N}\right) p_{(0,1)}(q_j) \\ &= \prod_{j=1}^N \frac{1}{\sqrt{1 - ik \frac{2D_j}{N}}}. \end{aligned} \quad (13)$$

From the characteristic function Eq. (13) the cumulants of the distribution

$$\kappa_m = \frac{1}{i^m} \frac{\partial^m \ln G_{\mathbf{D}}^{Nd}(k)}{\partial k^m} \Big|_{k=0} = \frac{2^{m-1}(m-1)!}{N^m} \sum_{i=1}^N D_i^m \quad (14)$$

are calculated for $m > 0$. The moments are recursively related to the cumulants by

$$M_m = \kappa_m + \sum_{k=1}^{m-1} \binom{m-1}{k-1} \kappa_k M_{m-k}. \quad (15)$$

It should be noted from Eq. (13) that the characteristic function is a product of independent functions in Fourier space. Hence, the distribution of diffusivities of an N -dimensional anisotropic system is determined by inverse Fourier transform of the characteristic function $p_{\mathbf{D}}^{Nd}(D) = \mathcal{F}^{-1} [G_{\mathbf{D}}^{Nd}(k)] = \mathcal{F}^{-1} [\prod_{i=1}^N G_{D_i/N}^{1d}(k)]$, where $G_{D_i/N}^{1d}(k) = \mathcal{F} [p_{D_i/N}^{1d}(D)]$ is the Fourier transform of the one-dimensional distribution of diffusivities $p_{D_i/N}^{1d}(D) = 1/\sqrt{2\pi D D_i/N} \exp(-ND/(2D_i))$ with diffusion coefficient D_i/N . Correspondingly, it is obtained by convolution of N one-dimensional distributions of diffusivities

$$\begin{aligned} p_{\mathbf{D}}^{Nd}(D) &= \{p_{\frac{1}{N}D_1}^{1d} * p_{\frac{1}{N}D_2}^{1d} * \dots * p_{\frac{1}{N}D_N}^{1d}\}(D) \\ &= \int_0^\infty d\Delta_1 \dots \int_0^\infty d\Delta_N \\ &\quad \times \delta \left(D - \sum_{i=1}^N \Delta_i \right) \prod_{j=1}^N p_{\frac{1}{N}D_j}^{1d}(\Delta_j), \end{aligned} \quad (16)$$

which follows directly from Eq. (10). Thus, with Eqs. (10), (13) and (16), we provide three analogous expressions to determine the distribution of diffusivities in terms of the eigenvalues D_i of \mathbf{D} . Depending on the considered system each representation offers its own advantages.

C. Asymptotic decay

In the following, we present the asymptotic behavior of the distribution of diffusivities for homogeneous anisotropic Brownian motion. We show how it allows identifying the anisotropy of the process.

Considering an M -fold degeneracy of the largest diffusion coefficient with $D_1 = \dots = D_M > D_{M+1} \geq \dots \geq D_N$ the distribution of diffusivities of the homogeneous anisotropic system is obtained from the convolution

$$p_{\mathbf{D}}^{Nd}(D) = \{p_{\frac{1}{N}D_1}^{Nd} * p_{\frac{1}{N}D_{M+1}}^{1d} * \dots * p_{\frac{1}{N}D_N}^{1d}\}(D), \quad (17)$$

where $p_{\frac{1}{N}D_1}^{Nd}(D)$ is the distribution of diffusivities of the M -dimensional isotropic system Eq. (7) with diffusion coefficient $D_c = D_1/N$, which results from the convolution of M identical one-dimensional distributions $p_{D_1/N}^{1d}(D)$.

For $D \gg D_1 D_{M+1} / (D_1 - D_{M+1})$ an approximation is introduced and yields the asymptotic behavior of Eq. (17)

$$\begin{aligned} p_{\mathbf{D}}^{Nd}(D) &\xrightarrow{D \rightarrow \infty} \left(\frac{N}{2D_1} \right)^{\frac{M}{2}} \frac{D^{\frac{M}{2}-1}}{\Gamma(\frac{M}{2})} \\ &\quad \times \exp \left(-\frac{N}{2D_1} D \right) \prod_{j=M+1}^N \sqrt{\frac{D_1}{D_1 - D_j}}. \end{aligned} \quad (18)$$

Thus, the general behavior in the logarithmic representation is governed by

$$\log p_{\mathbf{D}}^{Nd}(D) \xrightarrow{D \rightarrow \infty} -\frac{N}{2D_\infty} D, \quad (19)$$

which corresponds to the asymptotic decay of an N -dimensional, isotropic distribution of diffusivities with $D_\infty = \max(D_1, D_2, \dots, D_N)$, i.e., an exponential decay involving the largest diffusion coefficient of the anisotropic system.

In the homogeneous isotropic system D_∞ describing the asymptotic decay is equal to the isotropic diffusion coefficient D_c , cf. Eq. (7), which further coincides with the first moment $\langle D \rangle$. This is in contrast to the anisotropic case, where $\langle D \rangle < D_\infty$. Thus, the deviation of $\langle D \rangle$ and D_∞ offers a measure to characterize the anisotropy of the process by

$$\eta = \frac{D_\infty}{\langle D \rangle} - 1. \quad (20)$$

In cases where both values coincide, i.e., the system is isotropic, η becomes zero. On the contrary, if one diffusion coefficient is large compared to the others, $\langle D \rangle = D_\infty/N$ resulting in $\eta = N-1$, which denotes the largest possible anisotropy in N dimensions. Thus, η is a measure of the anisotropy, but it is not suitable to compare systems of different dimensionality N . It should be noted that similar measures with different ranges exist [15, 24].

For experimental data, the decay for large D is obtained from a fit to $f(D) = c \exp(-\lambda_{\text{fit}} D)$ to calculate $D_\infty = N/(2\lambda_{\text{fit}})$. The actual dimensionality M of processes observed in $N \geq M$ dimensions is estimated with $M = 2 \langle D \rangle \lambda_{\text{fit}}$ and, thus, the anisotropy is $\eta = N/M - 1$. For example, if an observed N -dimensional motion yields the largest anisotropy value of $\eta = N-1$, the process is effectively a one-dimensional motion.

D. Reconstruction of \mathbf{D}

For experiments it is of great interest to reconstruct the diffusion tensor \mathbf{D} from the measurements. If complete information about the trajectories is available, the diffusion tensor of the homogeneous anisotropic process can be estimated via the displacements. By defining tensorial diffusivities analogously to Eq. (4)

$$D_t^{ij}(\tau) = \frac{[x_i(t+\tau) - x_i(t)][x_j(t+\tau) - x_j(t)]}{2\tau}, \quad (21)$$

where $x_i(t)$ denotes the i -th component of the N -dimensional trajectory $\mathbf{x}(t)$, the linear τ dependence of the mixed displacements is removed. These tensorial diffusivities are simply averaged

$$D_{ij} = \langle D_t^{ij}(\tau) \rangle \quad (22)$$

providing an estimator for the corresponding elements of \mathbf{D} . Here, $\langle \dots \rangle$ either denotes a time average or an ensemble average depending on the available data.

IV. PROJECTION TO AN M -DIMENSIONAL SUBSPACE

Due to experimental restrictions the complete trajectory is often not accessible but its projection on an M -dimensional subspace can be measured. Such processes are commonly known as observed diffusion [25, 26].

The projection of the distribution of displacements Eq. (3) on the considered subspace is the marginal probability density

$$p(\mathbf{r}_\alpha^M, \tau) = \int d\mathbf{r}_{\alpha_1} \cdots \int d\mathbf{r}_{\alpha_{N-M}} p(\mathbf{r}, \tau), \quad (23)$$

where $r_{\alpha_i}, i = 1, \dots, (N - M)$ denotes $(N - M)$ arbitrarily chosen directions which are integrated out. The vector $\alpha = (\alpha_1 \dots \alpha_{N-M})$ contains the indices α_i describing which elements of \mathbf{r} are omitted. Alternatively, the projected distribution of displacements is computed by the M -dimensional inverse Fourier transform of the characteristic function of $p(\mathbf{r}, \tau)$ where the components, $k_{\alpha_i} = 0, \forall i \in \{1, \dots, N - M\}$, which correspond to the chosen directions, are discarded. Hence, the distribution of displacements of the subspace is

$$p(\mathbf{r}_\alpha^M, \tau) = \int d^M \mathbf{k}_\alpha^M \frac{1}{(2\pi)^M} \exp \left[-i(\mathbf{k}_\alpha^M)^\top \mathbf{r}_\alpha^M \right] G(\mathbf{k}_\alpha^M) \quad (24)$$

with the characteristic function of the projected propagator $G(\mathbf{k}_\alpha^M) = \exp[-(\mathbf{k}_\alpha^M)^\top \Sigma_\alpha^M \mathbf{k}_\alpha^M]$. The vector \mathbf{k}_α^M is an M -dimensional sub-vector of the complete k -space and Σ_α^M denotes a principal $M \times M$ submatrix of Σ obtained by deletion of rows and columns with same respective index α_i .

The distribution of diffusivities of such a projected diffusion process is calculated analogously to Eq. (6) by integrating over \mathbf{r}_α^M . Since $\Sigma = 2\tau\mathbf{D}$ is a symmetric, positive definite matrix for $\tau > 0$, all principal submatrices Σ_α^M are symmetric, positive definite matrices as well. Hence, they can be diagonalized and, thus, the projected distribution of diffusivities has the M -dimensional form of the generic expression Eq. (10), (13) or (16). However, it depends on the eigenvalues $D_{k,\alpha}^M, k = 1, \dots, M$ of the projected diffusion tensor $\mathbf{D}_\alpha^M = \Sigma_\alpha^M / (2\tau)$. If the eigenvalues of \mathbf{D} are identified as

$$D_1 \geq D_2 \geq \dots \geq D_N \quad (25)$$

and the eigenvalues of $\mathbf{D}_{(\alpha)}^{N-1}$ are

$$D_{1,(\alpha)}^{N-1} \geq D_{2,(\alpha)}^{N-1} \geq \dots \geq D_{N-1,(\alpha)}^{N-1}, \forall \alpha \in \{1, \dots, N\}, \quad (26)$$

the well-known interlacing inequalities [27] require

$$D_k \geq D_{k,(\alpha)}^{N-1} \geq D_{k+1}, \forall k \in \{1, \dots, N-1\} \quad (27)$$

for all $\alpha \in \{1, \dots, N\}$. This expression is applied recursively $(N-M)$ times to obtain a relation for the eigenvalues of the principal $M \times M$ submatrix [28]

$$D_k \geq D_{k,\alpha}^M \geq D_{k+N-M}, \forall k \in \{1, \dots, M\} \quad (28)$$

for arbitrary α . By implication, if at least two eigenvalues of the submatrix \mathbf{D}_α^M differ, i.e., the projected process is anisotropic, Eq. (27) states recursively that the complete process is anisotropic as well. Thus, the distribution of diffusivities of the projected N -dimensional anisotropic Brownian motion may already indicate the anisotropy of the complete process as well as the magnitude of one of the involved diffusion coefficients. However, a single projection is not sufficient to obtain the underlying diffusion coefficients.

Nevertheless, it is possible to estimate the bounds of the diffusion coefficients. The lower bound of the eigenvalues is given by zero, due to the positive semidefiniteness of \mathbf{D} . An upper bound for the largest eigenvalue can be found if enough projections or submatrices are available to cover the whole trace of \mathbf{D} . By use of the relation between the trace of an $N \times N$ matrix \mathbf{A} and its eigenvalues λ_i , $\text{tr } \mathbf{A} = \sum_i \lambda_i$, subtotals of the trace of \mathbf{D} are given by the sum of the eigenvalues of the respective submatrices. If the non-overlapping orthogonal projections of \mathbf{D} defined by α compose a partition of the set $\{1, \dots, N\}$, the trace of the tensor is given by

$$\text{tr } \mathbf{D} = \sum_{i=1}^N D_i = \sum_{\alpha} \text{tr } \mathbf{D}_\alpha^M = \sum_{\alpha} \sum_k D_{k,\alpha}^M \quad (29)$$

with $\dot{\bigcup} \alpha = \{1, \dots, N\}$, where the partition elements α do not necessarily have identical dimensionality.

For example, if one measures the eigenvalues of two non-overlapping projections of a 3×3 diffusion tensor \mathbf{D} , the trace of \mathbf{D} is given by

$$\begin{aligned} \text{tr } \mathbf{D} &= \text{tr } \mathbf{D}_{(1,3)}^1 + \text{tr } \mathbf{D}_{(2)}^2 \\ &= D_{1,(1,3)}^1 + D_{1,(2)}^2 + D_{2,(2)}^2. \end{aligned} \quad (30)$$

Thus, the eigenvalue inequalities for that example using the relations above are given by

$$\begin{aligned} \text{tr } \mathbf{D} &\geq D_1 \geq \max(D_{1,(1,3)}^1, D_{1,(2)}^2) \geq D_2 \\ D_2 &\geq \min(D_{1,(1,3)}^1, D_{2,(2)}^2) \geq D_3 \geq 0, \end{aligned} \quad (31)$$

which allows a rough estimation of the diffusion coefficients from the given projections.

V. SPECIFIC SYSTEMS

A. Two-dimensional systems

The distribution of diffusivities of a two-dimensional homogeneous anisotropic system is calculated, for instance, via Eq. (16), resulting in

$$\begin{aligned} p_{\mathbf{D}}^{2d}(D) &= \int_0^\infty d\Delta_1 \int_0^\infty d\Delta_2 \delta[D - (\Delta_1 + \Delta_2)] \\ &\times p_{\frac{1}{2}D_1}^{1d}(\Delta_1) p_{\frac{1}{2}D_2}^{1d}(\Delta_2) \\ &= \frac{\exp\left[-\frac{1}{2}\left(\frac{1}{D_1} + \frac{1}{D_2}\right)D\right]}{\sqrt{D_1 D_2}} I_0\left[\frac{1}{2}\left(\frac{1}{D_1} - \frac{1}{D_2}\right)D\right] \end{aligned} \quad (32)$$

where $I_0(x)$ denotes a modified Bessel function of the first kind. The first two moments of this distribution, as given by Eq. (8), yield

$$\langle D \rangle = M_1 = \frac{1}{2}(D_1 + D_2) \quad (33)$$

and

$$\langle D^2 \rangle = M_2 = \frac{1}{4}(3D_1^2 + 2D_1 D_2 + 3D_2^2). \quad (34)$$

Hence, the mean diffusion coefficient coincides with the arithmetic mean of the diffusion coefficients belonging to the two directions of the anisotropic system as expected from Eq. (12). Solving the simultaneous Eqs. (33) and (34) yields the expression

$$D_{1,2} = M_1 \pm \sqrt{M_2 - 2M_1^2} \quad (35)$$

to obtain the diffusion coefficients D_1 and D_2 from the moments.

The asymptotic behavior of Eq. (32) for large D is given by Eq. (18) and yields

$$p_{\mathbf{D}}^{2d}(D) \xrightarrow{D \rightarrow \infty} \frac{\exp\left(-\frac{D}{D_\infty}\right)}{\sqrt{|D_1 - D_2|} \pi D} \quad (36)$$

with $D_\infty = \max(D_1, D_2)$. Thus, the behavior in the logarithmic representation is governed by

$$\log p_{\mathbf{D}}^{2d}(D) \xrightarrow{D \rightarrow \infty} -\frac{D}{D_\infty}, \quad (37)$$

which corresponds to the decay of the distribution of diffusivities in two-dimensional homogeneous isotropic systems with D_∞ , i.e., an exponential decay with the largest diffusion coefficient of the anisotropic system. Accordingly, the smallest diffusion coefficient is given by $2\langle D \rangle - D_\infty$. From the asymptotic decay and the mean

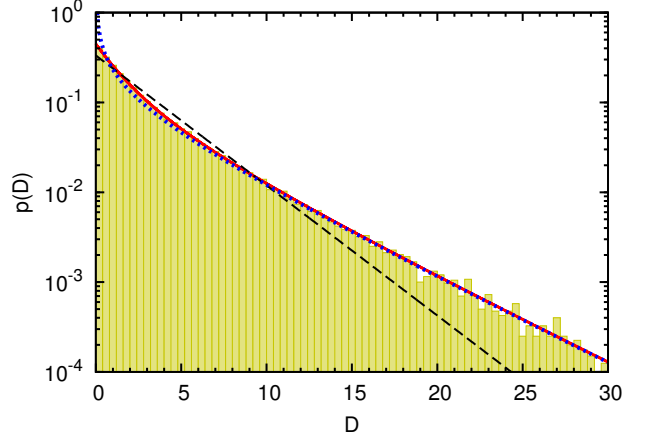


Figure 1. The distribution of diffusivities (histogram) from a simulated trajectory of a homogeneous anisotropic diffusion process in two dimensions with diffusion tensor \mathbf{D} given by Eq. (39) agrees well with the analytic distribution of diffusivities (solid line) from Eq. (32) with $D_1 = 5$ and $D_2 = 1$ denoting the eigenvalues of \mathbf{D} . Additionally, the asymptotic function Eq. (36) (dotted line, $D_\infty = 5$) agrees reasonably for large D . Furthermore, a distribution of diffusivities (dashed line) of two-dimensional isotropic diffusion with the same average diffusion coefficient $D_c = \langle D \rangle = (D_1 + D_2)/2 = 3$ is shown for comparison.

diffusion coefficient the anisotropy of the system is characterized by Eq. (20) and corresponds to the ratio

$$\eta = \frac{|D_1 - D_2|}{D_1 + D_2} = \frac{\sqrt{M_2 - 2M_1^2}}{M_1}, \quad (38)$$

which is also related to the moments.

To substantiate our analytical expressions by results from simulation, a random walk was performed by numerical integration of the Langevin equation Eq. (2) in two dimensions using the diffusion tensor

$$\mathbf{D} = \begin{pmatrix} 4 & \sqrt{3} \\ \sqrt{3} & 2 \end{pmatrix} \quad (39)$$

with the eigenvalues $D_1 = 5$ and $D_2 = 1$. The obtained trajectory of two-dimensional homogeneous anisotropic diffusion consisted of 10^5 displacements and its distribution of diffusivities is depicted in Fig. 1. The agreement of the normalized histogram from simulated data with the analytic distribution Eq. (32) is obvious. Deviations between simulation and the analytic curve for large D are due to insufficient statistics from the finite number of displacements. Moreover, Fig. 1 shows the monoeponential behavior corresponding to isotropic diffusion in two dimensions for comparison. Although the average diffusion coefficients of both processes coincide, the decays of the distributions differ. The reason is the asymptotic behavior given by Eq. (36) in the anisotropic case which exponentially decays with the largest eigenvalue for large D as depicted in the figure. In contrast, for

the isotropic system the asymptotic decay corresponds to the mean diffusion coefficient resulting in the quantitative difference. Furthermore, the distributions are qualitatively different for small D . A characteristic difference between the systems is the convex shape in the logarithmic representation of the anisotropic distribution of diffusivities. This intuitively results from the two different exponential decays related to the distinct diffusion coefficients D_1 and D_2 . In a more rigorous way, since $\frac{d^2}{dD^2} \log p_{\mathbf{D}}^{2d}(D) > 0$, the anisotropic distribution of diffusivities is a superconvex function [29].

For experimental data, it is easy to calculate the first two moments M_1 and M_2 by averaging the short-time diffusivities of Eq. (4) and their squares, respectively. The averaging is accomplished either along a single trajectory or from an ensemble of trajectories avoiding any numerical fit. The first two moments are sufficient to calculate D_1 and D_2 by Eq. (35).

For the sample trajectory used in Fig. 1 the first two moments are determined to be $\tilde{M}_1 = 2.987$ and $\tilde{M}_2 = 21.72$. According to Eq. (35), the underlying diffusion coefficients yield $\tilde{D}_1 = 4.956$ and $\tilde{D}_2 = 1.018$. These values agree well with the eigenvalues of the tensor Eq. (39), which was used as input parameter of the simulation. The calculation of $\eta = 2/3$ indicates a considerable anisotropy of the process.

1. Limiting cases

In the case of identical diffusion coefficients for both directions the anisotropy vanishes as discussed for Eq. (38). The resulting isotropic diffusion process is characterized by a single diffusion coefficient $D_c = D_1 = D_2$. Hence, Eq. (32) simplifies to the well-known distribution of single-particle diffusivities of two-dimensional isotropic diffusion [18]

$$p_{D_c}^{2d}(D) = \frac{\exp\left(-\frac{D}{D_c}\right)}{D_c} \quad (40)$$

given by an exponential function.

If, on the contrary, the anisotropy is large, diffusion in one direction will be suppressed. Without loss of generality, this is accomplished by tending one of the diffusion coefficients to zero. Thus, by taking the limit of vanishing D_2 , the distribution of diffusivities Eq. (32) is simplified to

$$p_{D_1}^{1d}(D) = \lim_{D_2 \rightarrow 0} p_{\mathbf{D}}^{2d}(D) = \frac{\exp\left(-\frac{D}{D_1}\right)}{\sqrt{\pi D_1 D}}, \quad (41)$$

which has the structure of the distribution of diffusivities of one-dimensional diffusion [18]. Since diffusion into the perpendicular direction is prohibited, as expected, it qualitatively leads to the observation of a one-dimensional process. This can be identified by the characteristic factor $D^{-1/2}$ due to which the distribution of

diffusivities diverges for small D . Applying Eq. (8) the first moment of Eq. (41), i.e., the mean diffusion coefficient, yields $\langle D \rangle = D_1/2$. The factor of 1/2 results from the single-particle diffusivities Eq. (4) with $N = 2$ assuming that a two-dimensional process is observed. However, due to the suppression of one direction this assumption is no longer valid and $N = 1$ should have been used instead. This conclusion is also obtained from the anisotropy value $\eta = 1$, which is equal to its maximum value for two-dimensional anisotropic processes since effectively one-dimensional motion is observed.

The alternative way to attain a large anisotropy would be to prefer diffusion in one direction by increasing the corresponding diffusion coefficient. Since there is always a contribution from the non-vanishing perpendicular direction, the distribution converges to $(D_1 D_2)^{-1/2}$ for small D . In the limit of an infinite diffusion coefficient, i.e., $D_1 \gg D_2$, a rescaling of D with $\langle D \rangle$ keeps the first moment constant and finally results in a behavior identical to Eq. (41).

2. Reconstruction of \mathbf{D}

In addition to the eigenvalues, it is sometimes of interest to determine the orientation of the principal axes of the system relative to the given frame of reference. This is achieved by the reconstruction of the diffusion tensor

$$\mathbf{D} = \begin{pmatrix} D_{11} & D_{12} \\ D_{12} & D_{22} \end{pmatrix}, \quad (42)$$

where the off-diagonal elements are labeled identically due to symmetry reasons. The reconstruction is accomplished in two ways either by considering the complete two-dimensional trajectory or by using one-dimensional projections of the trajectory.

In the first approach the tensorial diffusivities of Eq. (21) are used to obtain the tensor entries of \mathbf{D} . In accordance with Eq. (22) the tensor elements are estimated by averaging the tensorial diffusivities along a trajectory or over an ensemble. Moreover, the eigenvalues of tensor \mathbf{D} are expressed by its entries

$$D_{1,2} = \frac{1}{2} \left(D_{11} + D_{22} \pm \sqrt{(D_{11} - D_{22})^2 + 4D_{12}^2} \right) \quad (43)$$

and correspond to the diffusion coefficients of the system.

For the sample trajectory used in Fig. 1 the measured values \tilde{D}_{ij} yield the diffusion tensor

$$\tilde{\mathbf{D}} = \begin{pmatrix} 3.983 & 1.719 \\ 1.719 & 1.990 \end{pmatrix}, \quad (44)$$

which agrees reasonably with the input parameters of the simulation. The eigenvalues from this measured tensor $\tilde{D}_1 = 4.973$ and $\tilde{D}_2 = 1.000$ show a good agreement with the eigenvalues of the input tensor $D_1 = 5$ and $D_2 = 1$.

The second approach determines the tensor \mathbf{D} exclusively from one-dimensional projections of the trajectory.

In order to obtain results, at least three different projections are necessary. For simplicity, it is preferable to use projections along two perpendicular axes, which define the frame of reference for \mathbf{D} . Further, a projection onto an axis is required which is rotated about an angle θ relatively to the frame of reference. In such a setup, the first moments of the distribution of diffusivities related to the first two projections are identical to the averaged tensorial diffusivities $\langle D_t^{11}(\tau) \rangle$ and $\langle D_t^{22}(\tau) \rangle$. Thus, they yield the two diagonal elements of \mathbf{D} . The first moment of the third projection measures the leading diagonal element D_{11}^θ of the rotated tensor $\mathbf{D}^\theta = \mathbf{R}(\theta)^\top \mathbf{D} \mathbf{R}(\theta)$ with rotation tensor $\mathbf{R}(\theta) = \begin{pmatrix} \cos \theta & -\sin \theta \\ \sin \theta & \cos \theta \end{pmatrix}$. This additional value is sufficient to obtain the off-diagonal element of \mathbf{D} from

$$D_{12} = \frac{D_{11}^\theta - D_{11} \cos^2 \theta - D_{22} \sin^2 \theta}{\sin(2\theta)}. \quad (45)$$

For the calculation, any projection of the trajectory onto an arbitrary one-dimensional axis, i.e., any θ , can be used except directions perpendicular or parallel to axes of the frame of reference, i.e., angles θ which are multiples of $\pi/2$. It should be noted that the reconstruction from the distribution of diffusivities of projected trajectories is possible although the definition of the diffusivities omit any directional information.

In the example with $\tilde{D}_{11} = 3.983$, $\tilde{D}_{22} = 1.990$ and a measured $\tilde{D}_{11}^{5\pi/12} = 2.983$, the off-diagonal element yields $D_{12} = 1.719$, which is in good agreement with the value $\sqrt{3} \approx 1.732$ appearing as input parameter of the simulation.

In conclusion, it depends on the constraints of the experiment which of both approaches is more practicable. In either way the complete diffusion tensor \mathbf{D} is reconstructed reasonably.

B. Three-dimensional systems

Analogous to the two-dimensional case, it is possible to calculate the distribution of diffusivities either by inverse Fourier transform of the general characteristic function Eq. (13) or by the convolution Eq. (16). In both cases the analytical integration cannot be performed completely. However, the integration can be accomplished numerically. By integrating two variables Eq. (16) is reduced

to

$$\begin{aligned} p_{\mathbf{D}}^{3d}(D) &= \int_0^\infty d\Delta_1 \int_0^\infty d\Delta_2 \int_0^\infty d\Delta_3 \delta[D - (\Delta_1 + \Delta_2 + \Delta_3)] \\ &\times p_{\frac{1}{3}D_1}^{1d}(\Delta_1) p_{\frac{1}{3}D_2}^{1d}(\Delta_2) p_{\frac{1}{3}D_3}^{1d}(\Delta_3) \\ &= \int_0^D d\Delta_1 \left(\frac{3}{2}\right)^{3/2} \frac{1}{\sqrt{\pi D_1 D_2 D_3 \Delta_1}} \\ &\times \exp\left\{-\frac{3}{4}\left[\left(\frac{1}{D_2} + \frac{1}{D_3}\right)(D - \Delta_1) + \frac{2\Delta_1}{D_1}\right]\right\} \\ &\times I_0\left[\frac{3}{4}\left(\frac{1}{D_3} - \frac{1}{D_2}\right)(D - \Delta_1)\right]. \end{aligned} \quad (46)$$

For further simplification, a series expansion of the modified Bessel function $I_0(x)$ can be applied, which allows performing the last integration. However, this only results in a converging sum, which cannot be simplified any further.

By using the general expression of the cumulants Eq. (14) and the relation between cumulants and moments Eq. (15), the first three moments of the distribution of diffusivities of three-dimensional homogeneous anisotropic diffusion processes are

$$M_1 = \frac{1}{3}(D_1 + D_2 + D_3), \quad (47)$$

$$M_2 = \frac{1}{9} [(D_1 + D_2 + D_3)^2 + 2(D_1^2 + D_2^2 + D_3^2)], \quad (48)$$

and

$$\begin{aligned} M_3 &= \frac{1}{9} [5D_1^3 + 3D_1^2(D_2 + D_3) \\ &+ D_1(3D_2^2 + 2D_2 D_3 + 3D_3^2) \\ &+ (D_2 + D_3)(5D_2^2 - 2D_2 D_3 + 5D_3^2)]. \end{aligned} \quad (49)$$

These expressions are similar to Eqs. (33) to (34) and relate the moments of the distribution of diffusivities to diffusion coefficients D_1 to D_3 of the anisotropic process. By solving the simultaneous Eqs. (47) to (49) the underlying diffusion coefficients are determined by the measured moments of the distribution. The solution comprises six triplets (D_1 to D_3), which are permutations of the three diffusion coefficients. Due to the cubic contributions in Eq. (49) the expressions are too large to show here but can be easily obtained.

The asymptotic behavior of Eq. (46) for large D is given by Eq. (18), which assumes $D_1 > D_2 > D_3$, and results in

$$p_{\mathbf{D}}^{3d}(D) \xrightarrow{D \rightarrow \infty} \frac{\sqrt{3D_1} \exp\left(-\frac{3D}{2D_1}\right)}{\sqrt{2\pi(D_1 - D_2)(D_1 - D_3)D}}. \quad (50)$$

Thus, the behavior in the logarithmic representation is determined by

$$\log p_{\mathbf{D}}^{3d}(D) \xrightarrow{D \rightarrow \infty} -\frac{3D}{2D_\infty}, \quad (51)$$

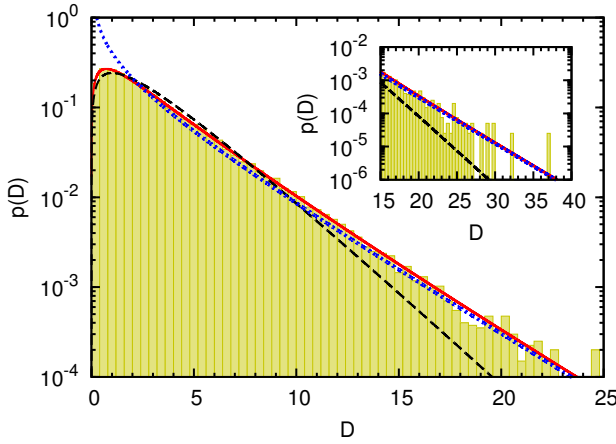


Figure 2. Distribution of diffusivities (histogram) from a simulated trajectory of a homogeneous anisotropic diffusion process in three dimensions with diffusion tensor \mathbf{D} given by Eq. (53) agrees well with the distribution of diffusivities (solid line) obtained from numerical integration of Eq. (46), using the eigenvalues $D_1 = 5$, $D_2 = 3$ and $D_3 = 1$ of tensor \mathbf{D} . For comparison, the distribution of diffusivities (dashed line) of an isotropic diffusion process in three dimensions, given by Eq. (54), is shown with the same average diffusion coefficient $D_c = \langle D \rangle = (D_1 + D_2 + D_3)/3 = 3$ as in the anisotropic process. In the inset, the asymptotic function Eq. (50) (dotted line, $D_1 = 5$) agrees reasonably for large D .

which corresponds to the asymptotic decay of a three-dimensional isotropic distribution of diffusivities with $D_\infty = \max(D_1, D_2, D_3)$. The anisotropy parameter Eq. (20) in the three-dimensional case corresponds to

$$\eta = \frac{(D_1 - D_2) + (D_1 - D_3)}{D_1 + D_2 + D_3}, \quad (52)$$

which considers the differences of the individual diffusion coefficients to characterize the anisotropy. It is obvious that the largest anisotropy yields $\eta = 2$.

In order to substantiate our results by simulated data, the simulation of a three-dimensional homogeneous anisotropic random walk was performed using the diffusion tensor

$$\mathbf{D} = \begin{pmatrix} 4 & -\frac{\sqrt{3}}{2} & -\frac{1}{2} \\ -\frac{\sqrt{3}}{2} & \frac{13}{4} & \frac{3\sqrt{3}}{4} \\ -\frac{1}{2} & \frac{3\sqrt{3}}{4} & \frac{7}{4} \end{pmatrix}. \quad (53)$$

The obtained trajectory consists of 10^5 displacements and its distribution of diffusivities is depicted in Fig. 2. The distribution of diffusivities from the simulated trajectory shows a good agreement with the curve obtained from numerical integration of Eq. (46). The deviations for larger values of D result from the finite simulation, i.e., its insufficient statistics. Furthermore, Fig. 2 shows the distribution of an isotropic system where a qualitative distinction at the crossover from the maximum peak to the exponential decay becomes apparent. In the isotropic

case the crossover in the logarithmic representation exhibits a concave curvature while in the anisotropic case it is convex after the peak. This is expected due to the different exponential decays related to the distinct diffusion coefficients D_1 to D_3 analogously to two-dimensional systems. However, a rigorous proof of $\frac{d^2}{dD^2} \log p_{\mathbf{D}}^{3d}(D) > 0$ for $D > D_{\text{peak}}$ is still missing. In addition, the asymptotic behavior given by Eq. (50) is depicted and provides a reasonable approximation for large D .

The eigenvalues of \mathbf{D} for experimental data are easily determined by measuring the leading moments of the diffusivities. For the sample trajectory used in Fig. 2 the first three moments result in $\tilde{M}_1 = 2.995$, $\tilde{M}_2 = 16.68$ and $\tilde{M}_3 = 140.2$. By solving the simultaneous Eqs. (47) to (49), the underlying diffusion coefficients yield $\tilde{D}_1 = 4.884$, $\tilde{D}_2 = 3.153$ and $\tilde{D}_3 = 0.948$. These values agree well with the eigenvalues of the tensor Eq. (53), which was used as input parameter of the simulation. The calculation of $\eta = 2/3$ indicates a considerable anisotropy of the process.

1. Limiting cases

If the diffusion coefficients of all three directions coincide with $D_c = D_1 = D_2 = D_3$, the distribution of diffusivities for the three-dimensional isotropic system [18]

$$p_{D_c}^{3d}(D) = 3 \sqrt{\frac{3}{2\pi} \frac{D}{D_c^3}} \exp\left(-\frac{3D}{2D_c}\right) \quad (54)$$

will be obtained from Eq. (46) in agreement with Eq. (7).

If exactly two diffusion coefficients coincide, one usually refers to diffusion processes of uniaxial molecules [20]. In this case, the general distribution of diffusivities of three-dimensional homogeneous anisotropic diffusion Eq. (46) simplifies to

$$p_{\text{uni}}^{3d}(D) = \frac{3}{2} \frac{\exp\left(-\frac{3D}{2D^{(2)}}\right) \text{erf}\left(\sqrt{\frac{3}{2}}\left(\frac{1}{D^{(1)}} - \frac{1}{D^{(2)}}\right)D\right)}{\sqrt{D^{(2)}(D^{(2)} - D^{(1)})}}, \quad (55)$$

where $D^{(1)}$ and $D^{(2)}$ are the eigenvalues of \mathbf{D} with multiplicity one and two, respectively. In general, a distinction between the oblate case ($D^{(2)} > D^{(1)}$, disc) and the prolate case ($D^{(2)} < D^{(1)}$, rod) is drawn for uniaxial molecules. In the prolate case both square roots in Eq. (55) yield complex numbers. However, with $\text{erf}(\sqrt{-x})/\sqrt{-y} = \text{erfi}(\sqrt{x})/\sqrt{y}$ for $x, y > 0$ and $x, y \in \mathbb{R}$, Eq. (55) remains a real valued function. Hence, a distinction between the two cases of the diffusion coefficients is not required for the distribution of diffusivities.

In the uniaxial case the first three moments simplify to

$$M_1 = \frac{1}{3}(D^{(1)} + 2D^{(2)}), \quad (56)$$

$$M_2 = \frac{1}{9}\left(3D^{(1)2} + 4D^{(1)}D^{(2)} + 8D^{(2)2}\right) \quad (57)$$

and

$$M_3 = \frac{1}{9} \left(5D^{(1)3} + 6D^{(1)2}D^{(2)} + 8D^{(1)}D^{(2)2} + 16D^{(2)3} \right). \quad (58)$$

Thus, the eigenvalues of \mathbf{D} are calculated by

$$D^{(1)} = M_1 \mp \sqrt{3M_2 - 5M_1^2} \quad (59)$$

and

$$D^{(2)} = M_1 \pm \frac{1}{2} \sqrt{3M_2 - 5M_1^2}, \quad (60)$$

where the sign in the equations depends on the constraint of positive diffusion coefficients. None of the eigenvalues will become complex since with Eqs. (56) and (57) the expression under the square root $3M_2 - 5M_1^2 = \frac{4}{9}(D^{(1)} - D^{(2)})^2 > 0$ is always positive and, hence, $M_2 > \frac{5}{3}M_1^2$. It should be noted that for $\frac{5}{3}M_1^2 < M_2 < 2M_1^2$ both signs in Eqs. (59) and (60) yield positive diffusion coefficients. In this case, the third moment has to be exploited in order to decide the correct pair of diffusion coefficients by comparing Eq. (58) with the measured value. Hence, there exist distributions of diffusivities with identical moments M_1 and M_2 , which result from different diffusion coefficients. In this case, the distinct M_3 determines the corresponding diffusion coefficients of the system. In the limit $M_2 \rightarrow \frac{5}{3}M_1^2$, $D^{(1)}$ and $D^{(2)}$ approach each other. In this particular case, the decision for the correct pair cannot be made accurately since both pairs yield approximately the same M_3 from Eq. (58). However, this limit corresponds to the isotropic system and, hence, the single diffusion coefficient is directly given by the first moment of the distribution.

Fig. 3 depicts examples of such distributions for the general anisotropic, the prolate, and the oblate case. The differences can be identified qualitatively. In the general and in the prolate case, the decay after the maximum peak has a convex curvature in the logarithmic representation, whereas in the oblate case it decays in a purely concave manner. This qualitative change is obtained from $\frac{d^2}{dD^2} \log p_{\text{uni}}^{3d}(D)$, where for $D^{(2)} > D^{(1)}$ this second derivative is always negative, i.e., $p_{\text{uni}}^{3d}(D)$ is a superconcave function. In the opposite case a zero-crossing is observed which results in a change from concave to convex curvature. However, a rigorous proof for the latter is still missing. In all cases, the exponential decay for large D is determined by the largest diffusion coefficient as given by Eq. (50). However, since the first decay after the peak is dominated by the smallest diffusion coefficient, the curve is shifted to the left for the prolate case in contrast to the oblate case when D_2 is changed from D_3 to D_1 . As expected from the first moment, the general case lies in between. A better distinction between the different cases is achieved quantitatively by determining the moments and calculating the diffusion coefficients.

In Fig. 4 the distribution of diffusivities for different ratios

$$r = D^{(1)}/D^{(2)} \quad (61)$$

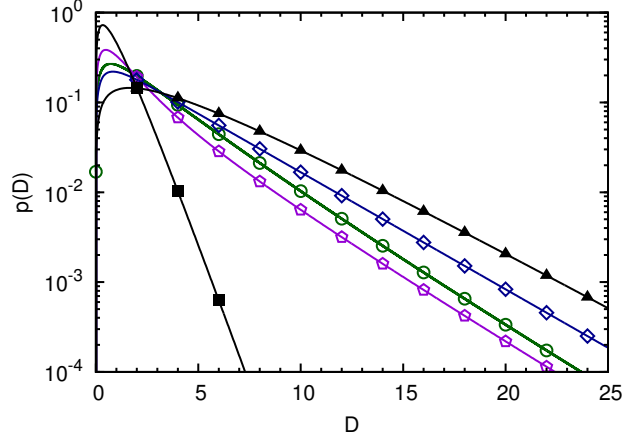


Figure 3. Distribution of diffusivities (lines with open symbols) of different homogeneous anisotropic diffusion processes in three dimensions. A qualitative distinction between the oblate case (\diamond ; $D^{(1)} = 1, D^{(2)} = 5$), the prolate case (\square ; $D^{(1)} = 5, D^{(2)} = 1$), and a general anisotropic case (\circ ; $D_1 = 5, D_2 = 3, D_3 = 1$) is possible since the decay after the maximum peak shows a concave curvature in the first case and a convex curvature in the latter cases. Furthermore, each anisotropic case obeys the same asymptotic decay given by the largest diffusion coefficient. For comparison the isotropic cases (lines with filled symbols) with $D_c = 1$ (\blacksquare) and $D_c = 5$ (\blacktriangle) are given, which always have a concave shape and, thus, are qualitatively indistinguishable from the oblate case.

is shown, ranging from oblate cases ($r < 1$) to prolate cases. It can be seen that in the limit $D^{(1)} \rightarrow 0$ and, thus, $r \rightarrow 0$, the distribution converges to the two-dimensional isotropic case with $D_c = 2/3D^{(2)}$. For $r \rightarrow 1$, the distribution converges to the three-dimensional isotropic case. In the prolate cases the distribution separates significantly from the three-dimensional isotropic case for increasing r . For further increasing ratios ($r \rightarrow \infty$) the distribution converges to the one-dimensional isotropic case with $D_c = 1/3D^{(1)}$. In contrast, the oblate cases converge rapidly to the two-dimensional isotropic case for decreasing r . A qualitative distinction may only be possible for small D , where the distribution still deviates from the mono-exponential behavior of the isotropic system. However, quantitatively the anisotropy is characterized by Eq. (20), which results in $\eta = \frac{1-r}{2+r}$ and $\eta = \frac{2(r-1)}{2+r}$ for oblate and prolate cases, respectively. Thus, in the oblate case the largest possible anisotropy emerges at small r , which yields $\eta = 1/2$ and clearly indicates the anisotropy. In the prolate case, the largest anisotropy will be obtained, if only one direction is preferred. Then, the anisotropy parameter $\eta = 2$ is maximal, which corresponds to one-dimensional motion in a three-dimensional system.

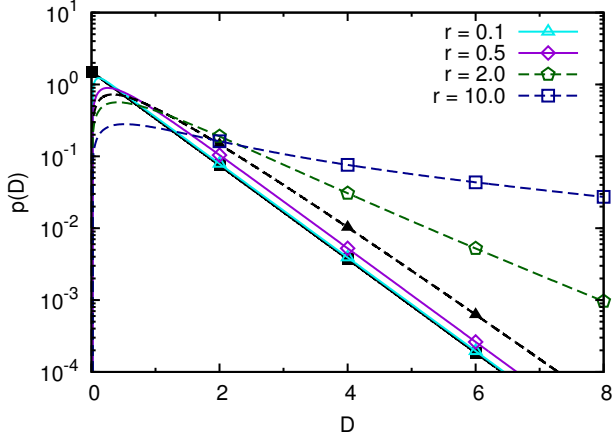


Figure 4. Distribution of diffusivities (lines with open symbols) for different ratios r given by Eq. (61) and fixed $D^{(2)} = 1$. The crossover from oblate cases ($r < 1$, solid lines) to prolate cases ($r > 1$, dashed lines) shows a broadening of the peak for increasing ratios. Again, the behavior after the peak changes from concave to convex, respectively. For comparison, the distribution of diffusivities of the limiting isotropic cases are depicted for two-dimensional (\blacksquare , $D_c = 2/3$) and three-dimensional processes (\blacktriangle , $D_c = 1$). The distinction of prolate cases from the isotropic limits is simpler than for the oblate cases.

2. Reconstruction of \mathbf{D}

As discussed for two-dimensional processes, the diffusion tensor will be easily obtained by measuring the averaged tensorial diffusivities according to Eq. (22) if the complete three-dimensional trajectory of the homogeneous anisotropic process is available. For the sample trajectory used in Fig. 2 the measured values \tilde{D}_{ij} yield the diffusion tensor

$$\tilde{\mathbf{D}} = \begin{pmatrix} 3.994 & -0.862 & -0.492 \\ -0.862 & 3.233 & 1.296 \\ -0.492 & 1.296 & 1.758 \end{pmatrix}, \quad (62)$$

which agrees reasonably with the input parameters of the simulation Eq. (53). Further, the eigenvalues from this measured tensor $\tilde{D}_1 = 4.983$, $\tilde{D}_2 = 2.998$ and $\tilde{D}_3 = 1.004$ show a good agreement with the eigenvalues of the input tensor $D_1 = 5$, $D_2 = 3$ and $D_3 = 1$.

However, if only a projection of the complete trajectory is available, e.g. from SPT, only the properties of the respective submatrix of \mathbf{D} can be measured. For instance, if the two-dimensional projection onto the x-y-plane of the sample trajectory is available, the first two moments of the distribution of diffusivities are determined to be $\tilde{M}_{1,z} = 3.613$ and $\tilde{M}_{2,z} = 26.95$. Using Eq. (35), the eigenvalues of the principal submatrix \mathbf{D}_z^2 are computed to be $\tilde{D}_{1,z}^2 = 4.531$ and $\tilde{D}_{2,z}^2 = 2.695$. Hence, the eigenvalue inequalities of Eq. (27) provide the estimate

$$D_1 \geq \tilde{D}_{1,z}^2 = 4.531 \geq D_2 \geq \tilde{D}_{2,z}^2 = 2.695 \geq D_3 \geq 0. \quad (63)$$

of the diffusion coefficients. As explained in Sec. IV, any further observed projection improves the estimates of the eigenvalues of \mathbf{D} . An additional projection onto the x-z-plane, for instance, yields the moments $\tilde{M}_{1,y} = 2.876$ and $\tilde{M}_{2,y} = 18.00$ resulting in the eigenvalues $\tilde{D}_{1,y}^2 = 4.083$ and $\tilde{D}_{2,y}^2 = 1.668$. Since with two orthogonal two-dimensional projections of the three-dimensional process the complete trace of \mathbf{D} is covered, an upper bound for the largest eigenvalue is found to be $D_1 \leq \text{tr } \mathbf{D} \leq \tilde{D}_{1,z}^2 + \tilde{D}_{2,z}^2 + \tilde{D}_{1,y}^2 + \tilde{D}_{2,y}^2 = 12.977$. Hence, the eigenvalue inequalities yield

$$\begin{aligned} 12.977 &\geq D_1 \geq \max(\tilde{D}_{1,z}^2, \tilde{D}_{1,y}^2) = 4.531 \\ \min(\tilde{D}_{1,z}^2, \tilde{D}_{1,y}^2) &= 4.083 \geq D_2 \geq \max(\tilde{D}_{2,z}^2, \tilde{D}_{2,y}^2) = 2.695 \\ \min(\tilde{D}_{2,z}^2, \tilde{D}_{2,y}^2) &= 1.668 \geq D_3 \geq 0. \end{aligned} \quad (64)$$

If additionally the projection onto the y-z-plane is available the eigenvalues of \mathbf{D} are estimated more precisely similar to the previous steps. To improve the upper bound of D_1 , the trace of \mathbf{D} is calculated from all these eigenvalues by $\text{tr } \mathbf{D} = \frac{1}{2}(\tilde{D}_{1,x}^2 + \tilde{D}_{2,x}^2 + \tilde{D}_{1,y}^2 + \tilde{D}_{2,y}^2 + \tilde{D}_{1,z}^2 + \tilde{D}_{2,z}^2)$, where the prefactor arises from the overlapping traces of the submatrices.

In case of the availability of all orthogonal two-dimensional projections of the process the tensorial diffusivities offer an advanced approach to determine the diffusion tensor. Since their first moments yield the entries of the principal submatrices \mathbf{D}_x^2 , \mathbf{D}_y^2 and \mathbf{D}_z^2 the underlying diffusion tensor \mathbf{D} is completely defined.

To summarize, the experimental setup influences the available data and affects how many parameters of the underlying process can be restored. A single two-dimensional projection may already hint at the anisotropy of the process. However, it is not sufficient to give an upper bound for the largest eigenvalue. An additional orthogonal two-dimensional projection or even a one-dimensional projection in the missing direction determines this upper bound and narrows the ranges of the eigenvalues. For a reconstruction of the complete tensor either the complete trajectory or three orthogonal two-dimensional projections of the process are necessary.

VI. CONCLUSIONS

To investigate N -dimensional homogeneous anisotropic Brownian motion we applied the distribution of diffusivities obtained from single-particle tracking data. From the general expression of the distribution of diffusivities we derived the relation of its moments and cumulants to the eigenvalues of the diffusion tensor \mathbf{D} . We showed that the asymptotic behavior of the distribution of diffusivities deviates from the isotropic case which allowed establishing an anisotropy measure based on the distribution. Since, due to experimental restrictions, often only projections of the trajectories are observed we further discussed the

consequences and provided an estimate for the bounds of the involved diffusion coefficients.

After our general considerations, we applied the results to specific systems with a high relevance in experiments. In particular, we investigated two-dimensional and three-dimensional systems as well as uniaxial molecules in three dimensions. In a two-dimensional homogeneous anisotropic system, the distribution of diffusivities comprises a modified Bessel function and allows a qualitative distinction from the mono-exponential decay observed in isotropic systems. Moreover, the first two moments of the distribution are sufficient to calculate the diffusion coefficients corresponding to the principal axes. Even the orientation of the principal axes and, thus, the complete diffusion tensor \mathbf{D} can be determined by using tensorial diffusivities or via three one-dimensional projections of the trajectory. For three-dimensional processes the general expression of the distribution of diffusivities is more elaborated and the last integration has to be evaluated numerically. However, we expressed the first three moments in terms of the diffusion coefficients belonging to the principal axes. Conversely, these expressions offer a method to calculate the diffusion coefficients from the moments measured in experiments, where other analysis fails. It is further shown that the isotropic and anisotropic systems differ in the logarithmic representation of the distribution of diffusivities, i.e., the asymptotic decay rate is proportional to the inverse slope of the msd and to the inverse of the largest diffusion coefficient, respectively. Thus, the distribution of diffusivities for anisotropic diffusion asymptotically decays slower than for isotropic diffusion with the same average diffusion coefficient. The deviation between the asymptotic decay and the decay belonging to the first moment provides a suitable measure for the anisotropy of the process. For uniaxial molecules diffusing in three dimensions the third integration is accomplished and the resulting distribution of diffusivities involves an error function. In this case, the diffusion coefficients of the principal axes depend on the first two moments of the distribution. For different ratios of the diffusion coefficients we distinguish between oblate and prolate cases, which show a concave and a convex

curvature in the logarithmic representation, respectively. Finally, we offer a guide to quantify the eigenvalues of \mathbf{D} from projected observations and to reconstruct the diffusion tensor in three dimensions from the moments of the tensorial diffusivities. The reconstruction from projected observations is possible although any directional information is discarded when determining the distribution of diffusivities.

In summary, the distribution of diffusivities provides an advanced analysis of anisotropic diffusion processes. The distribution is easily obtained from measured trajectories and allows for a characterization of the processes. Based on the distribution, anisotropic systems can be distinguished qualitatively from isotropic processes. Furthermore, from the moments of the distribution the diffusion coefficients can be reconstructed. Beyond that, the concept of diffusivities as scaled displacements is extended to tensorial diffusivities, which allow the reconstruction of the diffusion tensor from their first moments. Hence, the distribution of diffusivities complements well-established methods, such as mean squared displacements, for the analysis of diffusion data.

In future research, we will address the distinction between anisotropic and heterogeneous diffusion processes, which also involve more than one diffusion coefficient. Furthermore, since the eigenvalues of tensor \mathbf{D} are invariant to orthogonal transformations, we will apply our distribution of diffusivities to systems where the diffusion tensor changes its orientation in space and time, such as diffusion of ellipsoidal particles in isotropic media and diffusion in liquid crystalline systems with an inhomogeneous director field.

ACKNOWLEDGMENTS

We thank Sven Schubert for stimulating discussions and valuable suggestions. We gratefully acknowledge financial support from the Deutsche Forschungsgemeinschaft (DFG) for funding of the research unit FOR 877 “From Local Constraints to Macroscopic Transport”.

[1] N. G. van Kampen, *J. Phys. Chem. Solids* **49**, 673 (1988).

[2] M. Christensen and J. B. Pedersen, *J. Chem. Phys.* **119**, 5171 (2003).

[3] E. Bringuier, *Eur. J. Phys.* **32**, 975 (2011).

[4] B. Schulz, D. Täuber, F. Friedriszik, H. Graaf, J. Schuster, and C. von Borczyskowski, *Phys. Chem. Chem. Phys.* **12**, 11555 (2010).

[5] B. Schulz, D. Täuber, J. Schuster, T. Baumgärtel, and C. von Borczyskowski, *Soft Matter* **7**, 7431 (2011).

[6] J. Bechhoefer, J.-C. Gérinard, L. Bocquet, and P. Oswald, *Phys. Rev. Lett.* **79**, 4922 (1997).

[7] N. Wax, ed., *Selected Papers on Noise and Stochastic Processes* (Dover Publications, New York, 1954).

[8] M. J. Saxton and K. Jacobson, *Annu. Rev. Biophys.* **26**, 373 (1997).

[9] M. Dahan, S. Lévi, C. Luccardini, P. Rostaing, B. Riveau, and A. Triller, *Science* **302**, 442 (2003).

[10] D. T. Chen, E. R. Weeks, J. C. Crocker, M. F. Islam, R. Verma, J. Gruber, A. J. Levine, T. C. Lubensky, and A. G. Yodh, *Phys. Rev. Lett.* **90**, 108301 (2003).

[11] T. G. Mason, K. Ganesan, J. H. van Zanten, D. Wirtz, and S. C. Kuo, *Phys. Rev. Lett.* **79**, 3282 (1997).

[12] K. McHale, A. J. Berglund, and H. Mabuchi, *Nano Lett.* **7**, 3535 (2007).

[13] N. P. Wells, G. A. Lessard, and J. H. Werner, *Anal. Chem.* **80**, 9830 (2008).

[14] J.-H. Spille, T. Kaminski, H.-P. Königshoven, and U. Kubitscheck, *Opt. Express* **20**, 19697 (2012).

- [15] C. Ribrault, A. Triller, and K. Sekimoto, Phys. Rev. E **75**, 021112 (2007).
- [16] J. Kärger, D. M. Ruthven, and D. N. Theodorou, *Diffusion in Nanoporous Materials* (Wiley-VCH, Weinheim, 2012).
- [17] I. Hanasaki and Y. Isono, Physical Review E **85**, 051134 (2012).
- [18] M. Bauer, R. Valiullin, G. Radons, and J. Kärger, J. Chem. Phys. **135**, 144118 (2011).
- [19] C. Hellriegel, J. Kirstein, and C. Bräuchle, New J. Phys. **7**, 23 (2005).
- [20] P.-G. de Gennes and J. Prost, *The Physics of Liquid Crystals*, 2nd ed., International Series of Monographs on Physics, Vol. 83 (Clarendon Press, Oxford, 1995).
- [21] H. Risken, *The Fokker-Planck Equation: Methods of Solution and Applications*, 2nd ed., Springer Series in Synergetics, Vol. 18 (Springer, Berlin, 1989).
- [22] W. S. Price, *NMR Studies of Translational Motion*, Cambridge Molecular Science (Cambridge University Press, Cambridge, New York, 2009).
- [23] M. J. Saxton, Biophys. J. **72**, 1744 (1997).
- [24] S. Hess, D. Frenkel, and M. P. Allen, Mol. Phys. **74**, 765 (1991).
- [25] A. Dembo and O. Zeitouni, Stochastic Processes and their Applications **23**, 91 (1986).
- [26] F. Campillo and F. L. Gland, Stochastic Processes and their Applications **33**, 245 (1989).
- [27] A. L. Cauchy, in *Oeuvres complètes d'Augustin Cauchy* 2, Vol. 9 (Gauthier-Villars et fils, Paris, 1829) pp. 174–195.
- [28] K. Fan and G. Pall, Canad. J. Math. **9**, 298 (1957).
- [29] J. F. C. Kingman, Quart. J. Math. **12**, 283 (1961).